Available online at www.sciencedirect.com
ScienceDirect
Bioorganic & Medicinal Chemistry 15 (2007) 2690–2700
Bioorganic & Medicinal Chemistry

Optimization and determination of the absolute configuration of a series of potent inhibitors of human papillomavirus type-11 E1–E2 protein–protein interaction: A combined medicinal chemistry, NMR and computational chemistry approach

Nathalie Goudreau,[a,*] Dale R. Cameron,[a,†] Robert Déziel,[a,‡] Bruno Haché,[a] Araz Jakalian,[a] Eric Malenfant,[a] Julie Naud,[a] William W. Ogilvie,[a,§] Jeff O'Meara,[a] Peter W. White[b] and Christiane Yoakim[a]

[a]*Department of Chemistry, Boehringer Ingelheim (Canada) Ltd, Research & Development, 2100 Cunard Street, Laval, Que., Canada H7S 2G5*
[b]*Department of Biological Sciences, Boehringer Ingelheim (Canada) Ltd, Research & Development, 2100 Cunard Street, Laval, Que., Canada H7S 2G5*

Received 11 December 2006; revised 15 January 2007; accepted 19 January 2007
Available online 24 January 2007

Abstract—We have previously reported the discovery and initial SAR optimization of the first series of inhibitors of the human papillomavirus type-11 (HPV11) E1–E2 protein–protein interaction. These inhibitors featured an indandione system spiro-fused onto an all *syn* substituted tetrahydrofuran ring. In this paper, we report new SAR efforts which have led to the identification of the first low nanomolar inhibitor of the HPV11 E1–E2 protein–protein interaction. In addition, we report a combined NMR and computational chemistry approach which allowed the successful determination of the absolute stereochemistry of the active species originating from the initial racemic lead.
© 2007 Elsevier Ltd. All rights reserved.

1. Introduction

Papillomaviruses are a family of small double-stranded DNA viruses associated with a broad spectrum of diseases ranging from cutaneous and genital warts to anogenital cancer.[1] More than 25 types of human papillomaviruses (HPV) infect the anogenital region and these HPV types have been classified as 'low-risk' or 'high-risk' types depending on the particular pathologies they are associated with. For example, HPV6 and 11 cause benign genital warts (condyloma acuminata) and are the most common 'low-risk' types, whereas HPV16, -18, and -31 represent the most prevalent 'high-risk' types and are the major cause of cervical cancer.[1] Interestingly, the recent approval of a new vaccine targeting HPV types 6, 11, 16, and 18, referred to as Gardasil®, represents a significant breakthrough in women's health. Indeed, this vaccine was shown to be efficacious in decreasing the incidence of HPV infection, and thus of both genital warts and cervical cancer.[2] However, therapies to treat HPV-induced lesions include a variety of ablative or cytodestructive procedures as well as the use of the immunostimulator imiquimod.[3,4] These treatments are far from ideal and no specific small molecule antivirals are yet available for the treatment of HPV infections.

The HPV genome encodes eight well-characterized proteins, only two of which, E1 and E2, are required for DNA replication.[5] Viral DNA replication is initiated by the cooperative binding of E1 and E2 to specific DNA sequences within the HPV viral origin. Assembly of this E1–E2-origin complex is dependent on the

Keywords: Human papillomavirus; Protein–protein interaction; Indandione, NMR.
* Corresponding author. Tel.: +1 450 682 4640; fax: +1 450 682 4189; e-mail: ngoudreau@lav.boehringer-ingelheim.com
† Present addresses: Migenix; BC Research Building, 3650 Wesbrook mall, Vancouver, BC, Canada V6S 2L2.
‡ Methylgene, 7220 Frederick Banting #200, Montréal, Que., Canada H4S 2A1.
§ Department of chemistry, University of Ottawa, 10 Marie Curie, Ottawa, Ont., Canada K1N 6N5.

0968-0896/$ - see front matter © 2007 Elsevier Ltd. All rights reserved.
doi:10.1016/j.bmc.2007.01.036

binding of E2 to high affinity sites in the origin as well as on a critical protein–protein interaction between E1 and E2.[5,6] The essentiality of E1 and E2 in HPV DNA replication makes them attractive targets for novel antiviral therapies.

By screening our corporate compound collection we identified **1**, a molecule capable of antagonizing the protein–protein interaction between the E1 and E2 proteins of HPV11 (Fig. 1).[7,8] Specifically, this inhibitor featured an indandione system spiro-fused onto a substituted tetrahydrofuran ring and had an IC_{50} of 11 μM in our in vitro E1–E2-ori-complex formation assay.[9] Upon resynthesis and separation of the resulting diastereoisomers, the inhibitory activity of the original hit **1** was found to reside in the *syn/syn* isomer **2** (Fig. 1).[7] In addition, isothermal titration calorimetry and fluorescence studies showed that this series of inhibitors act by binding to the N-terminal transactivation domain (TAD) of E2, the region of the protein that interacts with E1.[6,8] Furthermore, these inhibitors were found inactive in a mechanistically related specificity assay that measures binding of SV40 large T antigen to its cognate origin.[8]

Early stability studies indicated however that compound **2** was readily converted in the binding assay buffer (sodium phosphate, pH 7.4) to other products. The structures of these new products were elucidated and the mechanism by which they were produced was determined using NMR and mass spectrometry techniques.[10] In particular, it was demonstrated that dissolution of inhibitor **2** in aqueous solutions at pH 7.0 or above resulted in the rapid and regioselective hydrolysis of its maleimide functionality to generate the corresponding carboxylate **4**. Moreover, this process was found to involve neighboring-group participation of the indandione ketone moiety via the formation of the intermediate hydroxylactone **5** (Fig. 2). Similar to the maleimide **2**, this latter derivative was also found to rapidly convert in the assay buffer to the carboxylate species **4**, in agreement with the comparable activity measured for all three compounds.[10]

Having established that the active form of our original hit was represented by **4**, we then undertook an initial SAR study. This first optimization process focused on the 4-chlorophenyl moiety of the inhibitor and showed that a 20-fold increase in potency could be obtained by the addition of another chloro substituent, as in **6** (Table 1).[7] In this paper, we will report further improvement to this series of inhibitors through novel SAR studies. In addition, we will describe the use of a combined NMR and computational chemistry approach which allowed the successful determination of the absolute configuration of the active enantiomer originating from the initial racemic lead.

2. Chemistry

The syntheses of compounds **2**–**21** were carried out according to Scheme 1, as previously described.[7,10] In brief, Knoevenagel condensation of indan-1,3-dione with the appropriately substituted benzaldehydes (di-chloro or di-bromo) in the presence of piperidine gave the corresponding benzylidene intermediates, which were treated with peroxide under basic conditions to give the corresponding epoxide derivatives **A**. Dipolar cycloaddition with different maleimide derivatives **B** in refluxing toluene gave a 1:1 mixture of the *syn/syn* adducts **C** and the *syn/anti* compounds **D**, which were readily separated by flash chromatography. The *syn/syn* derivatives **C** were finally converted to the corresponding sodium salts **E** by the slow addition of aqueous NaOH.

The epoxide derivative **K** necessary for the synthesis of compounds **22** and **23** is highlighted in Scheme 2.

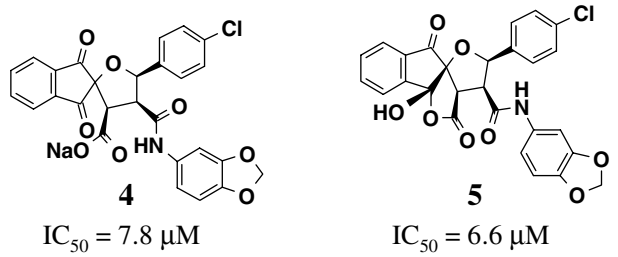

Figure 2. Structures and biological activities of the hydrolysis products of inhibitor **2**. Compounds are racemic.

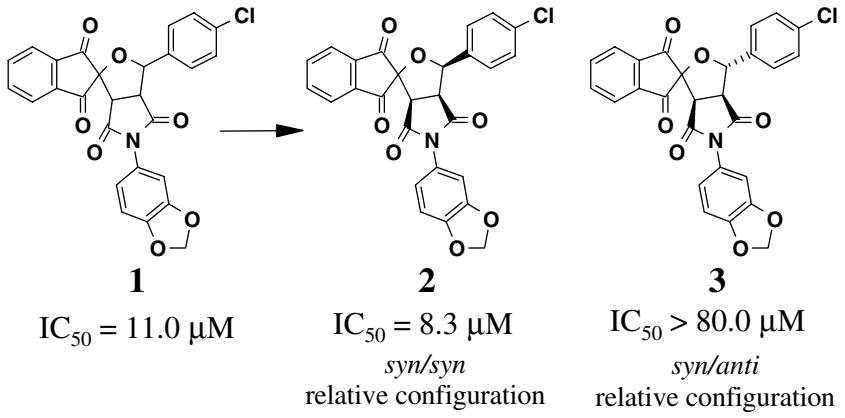

Figure 1. Structures of the initial lead inhibitors of E1–E2 protein–protein interaction. All compounds are racemic.

Table 1. Biological activities in the HPV11 in vitro E1–E2-ori-complex formation assay[8]

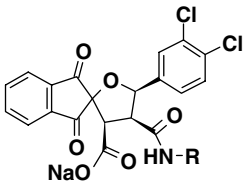

Compound[a]	R	IC_{50} (μM)
6	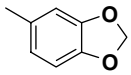	0.35
7		0.68
8		2.1
9[b]		3.5
10	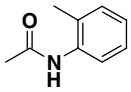	65.0
11	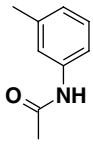	0.74
12	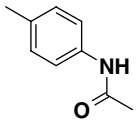	0.44
13	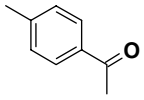	0.38
14	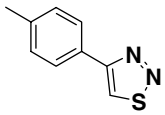	0.15
15	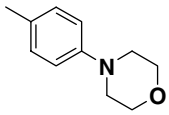	0.088

[a] All compounds are racemic.
[b] Prepared as the hydroxylactone form.

Homologation of commercially available aldehyde **F** with malonic acid followed by catalytic hydrogenation of the exocyclic double bond provided acid **H**. Cyclization under acidic condition gave intermediate **I** in 35% yield. Compound **I** was condensed with 3,4-dibromobenzaldehyde under acidic condition in benzene to generate compound **J** in moderate yield. Oxidation to the corresponding diketone followed by epoxidation of the double bond provided the required epoxy-diketone **K** in good yield. Further elaboration of this intermediate to inhibitors **22** and **23** was accomplished as highlighted in Scheme 1.

3. Results and discussion

Compound **6** was selected as the starting point of this new optimization, which mainly focused on the amide portion of the inhibitor. As shown in Table 1, replacement of the original 1,3-benzodioxol-5-yl amide moiety by a simple phenyl amide resulted in only a 2-fold loss in potency (**7**). However a more drastic loss in potency (6- or 10-fold) was observed when a *tert*-butyl group (**8**) or a benzyl amide derivative (**9**) was introduced. These early results suggested that anilide derivatives were overall preferred. Thus, starting from the anilide derivative **7**, a variety of substituents were next introduced onto its phenyl ring. The general trends revealed by this exercise can be summarized with the results of compounds **10**, **11**, and **12**. First, addition of substituents at the *ortho* position of the phenyl ring was found to be highly detrimental, as exemplified by the almost 100-fold loss in potency observed following the introduction of an *o*-methyl amide substituent (**10**). This observation was also true for a wide number of *ortho* substituents (not shown). Introduction of substituents at the *meta* position was in contrast better tolerated, as illustrated by the similar potency displayed by **11**. However, it is at the *para* position that substituents displayed the most beneficial effect, as exemplified with compounds **12**, **13**, **14**, and **15**. In addition, this position was found to be quite permissive since a wide variety of substituents were tolerated. Overall, the most significant gain was observed when different heterocycles were introduced such as the thiadiazole substituent (**14**) which displayed a 4-fold improvement in potency as compared to the unsubstituted reference analog **7**. Finally, the best *para* substituent we identified consisted in the morpholino moiety (**15**) which provided a further improvement in potency.

It is worth mentioning that all the inhibitors had been synthesized as racemic mixtures. We were therefore very interested to find out if both enantiomers were able to antagonize the E1–E2 protein–protein interaction to the same extent. To address this important issue, we first introduced on our current series of inhibitors an additional chiral center in order to generate a pair of diastereoisomers. Specifically, analogs of **9** containing a (*R*)-methyl benzyl amide derivative were prepared and successfully separated to provide two diastereoisomers (**16** and **17**) with the all-*syn* furan stereochemistry; the 'all-down' (2*S*,3*S*,4*R*,5*S*) and the 'all-up' (2*R*,3*R*,4*S*,5*R*) furan configuration, respectively (Fig. 3). Interestingly, only one of the two resulting diastereoisomers (**17**) was found to be active, displaying an IC_{50} of 6.8 μM. At this point, the absolute configuration of this active derivative remained unknown and we were consequently very interested in elucidating this matter.

In a previous study, we had demonstrated that under acidic conditions our inhibitors could be isolated as

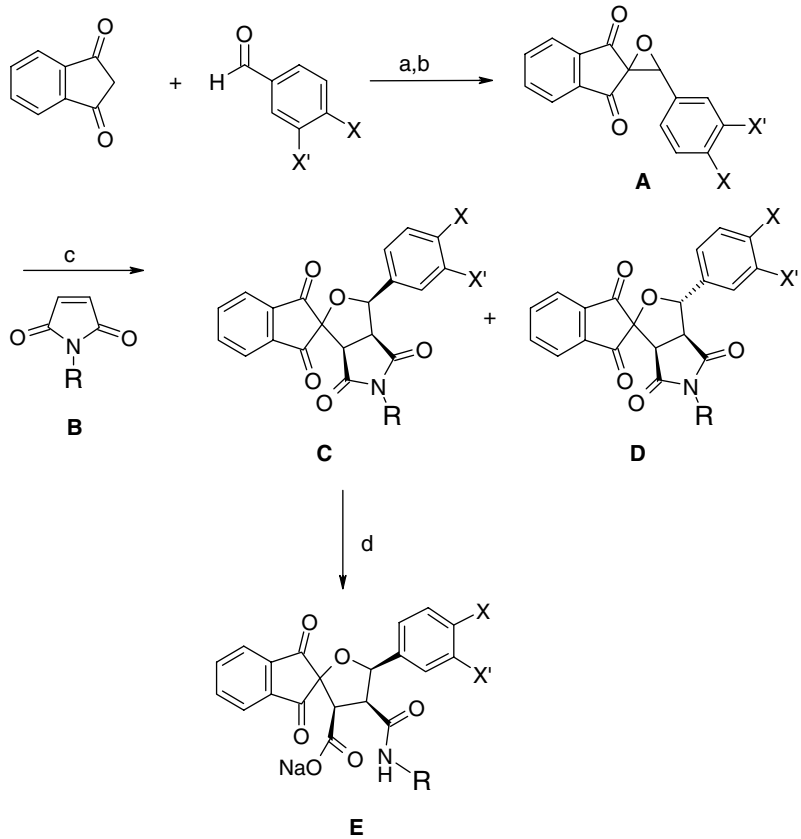

Scheme 1. Reagents and condition: (a) EtOH, piperidine (cat.); (b) H_2O_2, NaOH, MeOH; (c) toluene, reflux; (d) CH_3CN, NaOH slow addition; X = X′ = Cl or Br.

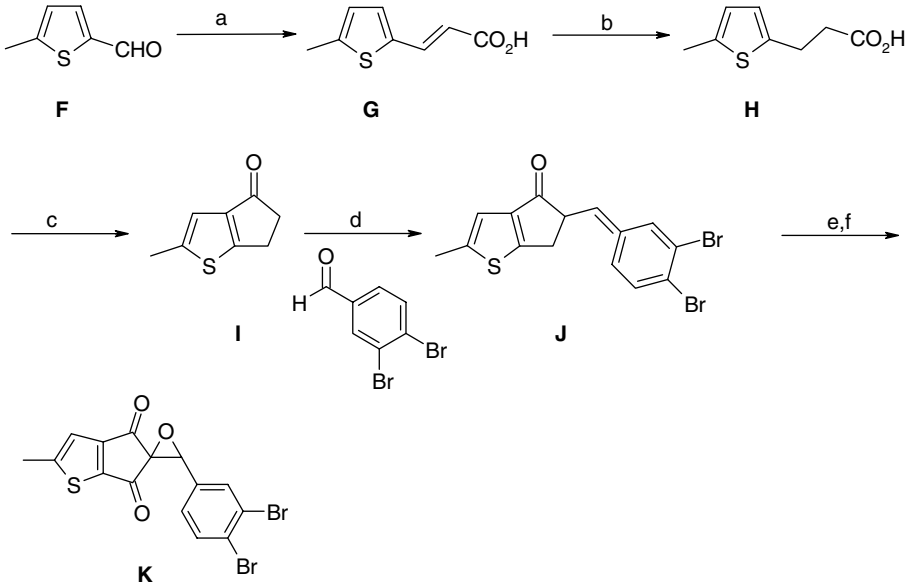

Scheme 2. Reagents and conditions: (a) malonic acid, piperidine/pyridine, reflux, H_2O, HCl, 100% yield; (b) $Pd(OH)_2$, EtOH, H_2, 93% yield; (c) polyphosphoric acid, 75 °C, 35% yield; (d) *p*-toluenesulfonic acid, benzene, reflux, 49% yield; (e) CrO_3, CH_2Cl_2, *tert*-butylhydroperoxide, 60% yield; (f) H_2O_2, NaOH, MeOH, 90% yield.

hydroxylactone intermediates (**5**, Fig. 2) through the involvement of one of the neighboring indandione ketones.[10] Although these intermediates were shown to rapidly convert in the assay buffer into their carboxylate counterparts, they were nevertheless stable enough to allow their isolation and full characterization in organic solvents.[10] Moreover, one interesting feature of these intermediates was the level of asymmetry they displayed, at least from an NMR viewpoint. Therefore, in order to establish the absolute configuration of the active

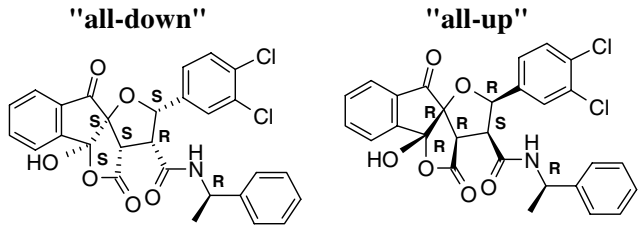

16 $IC_{50} > 75.0$ μM

17 $IC_{50} = 6.8$ μM

Figure 3. Structures and biological activities of the two chiral inhibitors used in the combined NMR and computational chemistry study.

diastereoisomer **17**, we carried out a combined NMR and computational chemistry approach that took advantage of the asymmetry and rigidity of the hydroxylactones, as well as to the presence of the remote chiral center of known stereochemistry. Indeed, we believed that this chiral center would confer sufficiently distinct conformational preferences to each of the diastereoisomers to allow their absolute configuration to be established.

The simple comparison of the 1D proton NMR spectra of the two hydroxylactone derivatives **16** and **17** in DMSO highlighted specific chemical shift differences. Most noticeable was the 0.5 ppm difference observed between their methyl resonances, as shown in Figure 4. This observation reflected the distinct local environment that this specific methyl group is experiencing in each compound, most probably as a result of their overall different conformational behavior. This difference was further confirmed through the recording of 1D NOE and 2D ROESY experiments. In case of compound **16**, we were able to observe that its 3,4-dichlorophenyl ring protons were having weak NOEs to those of the benzyl ring moiety, but not to those of the methyl group (Fig. 4). This was in contrast to what was observed for analog **17**, for which the 3,4-dichlorophenyl ring protons displayed specific weak NOEs to those of the methyl group but not to those of the benzyl moiety (supplementary material). Altogether, these results clearly demonstrated the different conformational behavior that these two diastereoisomers exhibit in solution.

The two hydroxylactone derivatives were also studied by molecular mechanics in order to determine their conformational preferences *in-silico* and establish a correlation with our experimental data. To begin, a systematic conformational search around key single bonds was performed for each compound using the MMFF94 forcefield within the MOE software package (Chemical Computing Group Inc., Montreal, Canada), which allowed the identification of a series of distinct low energy conformations (Table 2). The lowest energy conformation found for each diastereoisomer is shown in Figure 5. In addition, the distances between the center of the 3,4-dichlorophenyl ring (A) and both the centers of the benzyl ring (B) and of the methyl moiety (C) were measured for the five lowest energy conformations of each diastereoisomer (Table 3). Specifically for the 'all-down' diastereoisomer conformations, the distance between A and B was found to be shorter on average (4.7 Å) than the distance between A and C (6.2 Å). In contrast to the 'all-up' diastereoisomer conformations, the distance between A and C was found to be shorter on average (4.8 Å) than the average distance between A and B (6.7 Å). These data clearly highlighted the different conformational preferences that these two diastereoisomers exhibit *in-silico*. Interestingly when the computational and NMR results were compared, specific correlations could be established. For instance, the lowest energy conformation determined *in-silico* for the 'all-down' isomer was found to be consistent with the NOE information obtained for inhibitor **16** (inactive), while the lowest energy conformation of the

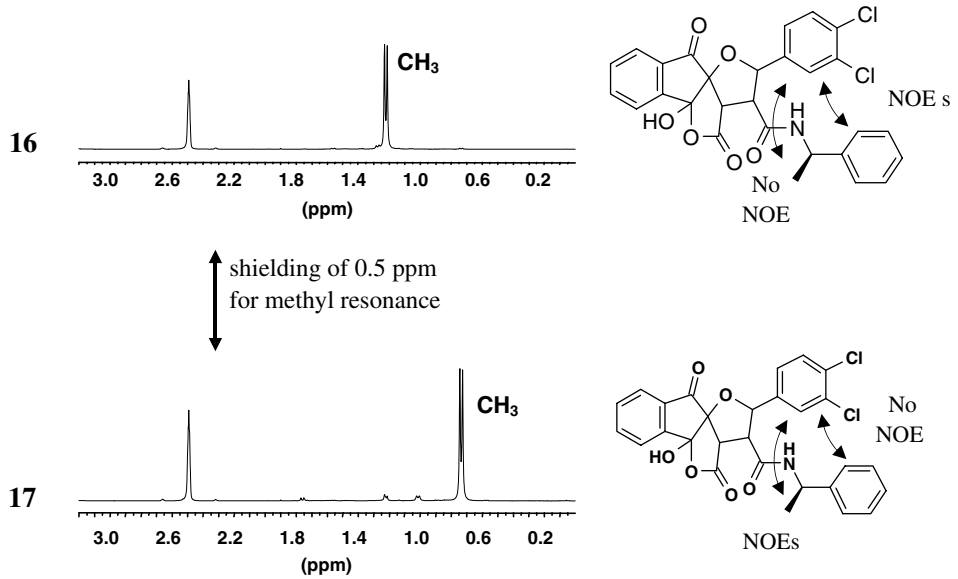

Figure 4. Subregion of ^{1}H NMR spectra and ROESY information of inhibitors **16** and **17**.

Table 2. Systematic conformational search of the two hydroxylactone derivatives **16** and **17**

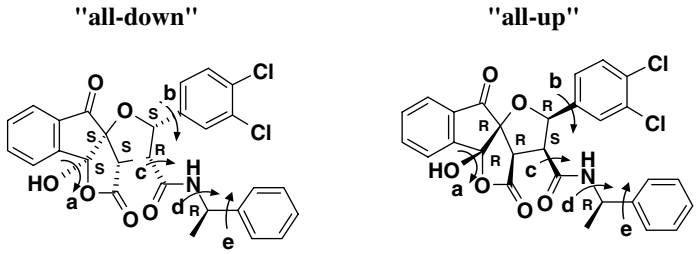

Conformers	Energy (kcal/mol)	Me–Phe distance (Å)	Phe–Phe distance (Å)
'all-down'			
1	67.8175	6.59	4.15
2	67.9376	6.30	4.82
3	69.2578	5.98	4.19
4	69.3113	6.71	6.08
5	69.6694	5.43	4.49
'all-up'			
1	69.0609	3.85	6.54
2	69.1739	3.95	6.78
3	69.3271	6.43	4.12
4	70.1207	4.75	7.99
5	70.2856	4.91	8.13

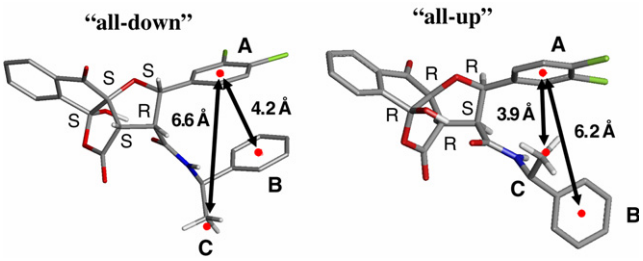

Figure 5. Lowest energy conformations of the two hydroxylactone diastereosiomers. For clarity some of the hydrogen atoms are omitted.

'all-up' isomer was found to be consistent with the NOE information obtained for inhibitor **17** (active). In addition, these conformations were also consistent with the 0.5 ppm up-field shift observed for the methyl resonances of **17**, since in the 'all-up' representative conformation the methyl moiety is directly positioned in the anisotropic shielding cone of the 3,4-dichlorophenyl ring (Fig. 5). Therefore, based on this combined NMR and computational chemistry study, we predicted that the active enantiomer **17** had the 2*R*,3*R*,4*S*,5*R* furan absolute configuration ('all-up'; Fig. 3). Subsequent to this study we obtained an X-ray co-crystal structure of inhibitor **18**, bound to the HPV11 E2 transactivation domain (Fig. 6).[11] In addition to identifying the binding pocket of this series of inhibitors, this X-ray structure unambiguously confirmed that the active enantiomer had the 3*R*,4*S*,5*R* furan absolute stereochemistry ('all-up') as correctly predicted (Fig. 6).

Further SAR investigations also allowed us to demonstrate that the 3,4-dichlorophenyl moiety could be replaced by its 3,4-dibromo counterpart giving rise to a moderate improvement in potency, as illustrated with **19** (IC_{50} = 0.051 μM, Fig. 7) when compared to **15** (IC_{50} = 0.088 μM, Table 1). In addition, since we knew

Table 3. Biological activities in the HPV11 in vitro E1–E2-ori-complex formation assay

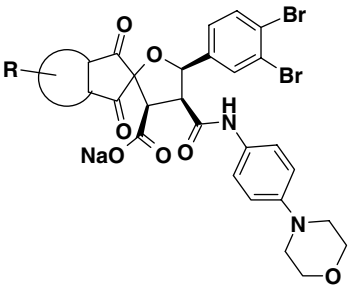

Compound[a]	R	IC_{50}(μM)
21	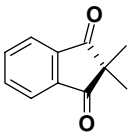	0.028
22	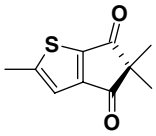	0.46
23	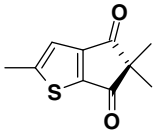	0.006

[a] Compounds are enantiomerically pure.

that most of the activity resided in one enantiomer, we then undertook the separation of racemic **19** using chiral HPLC in order to obtain the two enantiomerically pure inhibitors, the 3*R*,4*S*,5*R* ('all-up') and the 3*S*,4*R*,5*S* ('all-down') analogs, respectively. Again, we were quite pleased to see that isomer **20** ('all-down') was found to

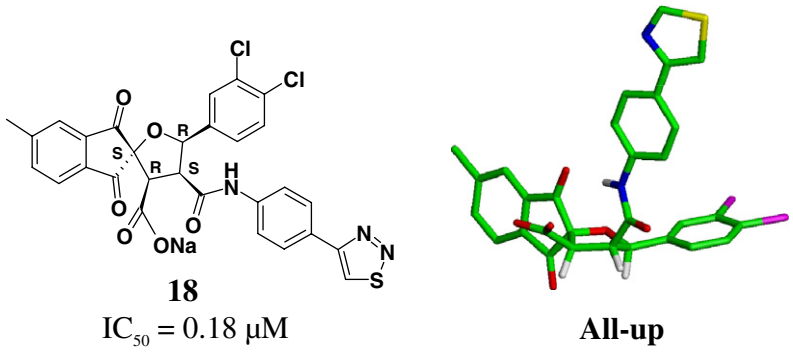

Figure 6. Bound conformation of inhibitor **18** to the HPV11 E2 transactivation domain derived from the X-ray co-crystal structure.[11]

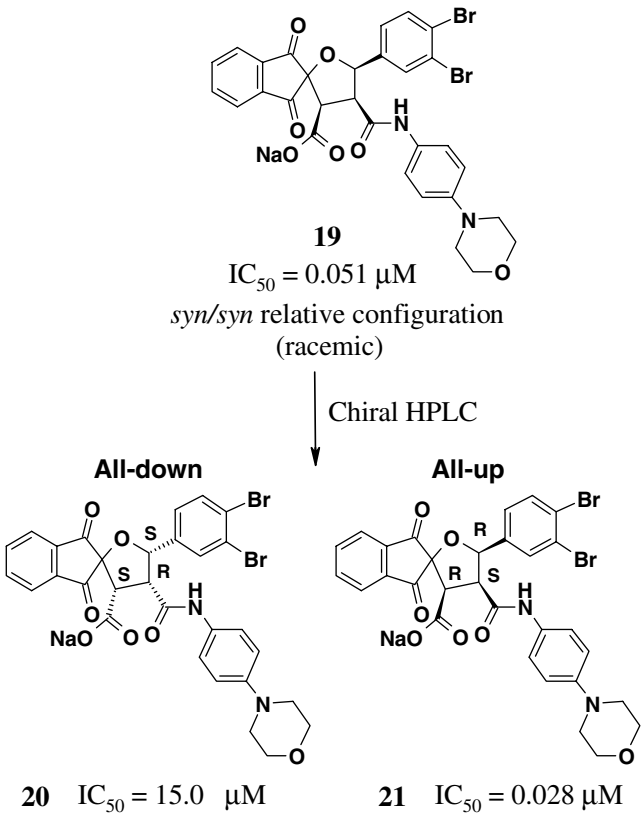

Figure 7. Structures and biological activities of the two enantiomerically pure inhibitors. The absolute configuration was assigned based on the X-ray co-crystal structure of analog **18**.[10]

be significantly less active, displaying an IC_{50} of 15 μM, as compared to the other enantiomer **21** ('all-up') which was found to be almost 2-fold more potent than the racemic mixture, with an IC_{50} of 0.028 μM. These data definitively illustrated the specific nature of the HPV11 E1–E2 protein–protein interaction that this class of inhibitors is able to antagonize.

Compound **21** was then selected as the starting point of a final optimization process, which focused on the indanedione portion of the inhibitor. Introduction of single small substituents (F, Me) at the different positions of its indane ring resulted in compounds that were either less potent or at best only marginally more potent (data not shown). The synthesis, purification, and characterization of these particular compounds became however quite challenging as the dipolar cycloaddition reaction yielded each time a mixture of two regioisomers (at the level of the indandione) in combination with a mixture of *syn/syn* and *syn/anti* tetrahydrofuran adducts (analogs **C** and **D**, Scheme 1) giving raise to a total of four possible diasteroisomeric pairs (each being racemic). The only substantial gain in potency that was observed during this exercise was when the original indandione portion was replaced by a cyclopentathiophene derivative, as shown in Table 3. Indeed, compound **23** (which is enantiomerically pure) displayed an IC_{50} of 0.006 μM which represented a 4.5-fold improvement over reference compound **21**. It is also interesting to note that the thiophene regiochemistry was found to be extremely important for the activity since regioisomer **22** was found to be 75-fold less potent than its regiocounterpart **23**. This again further highlights the specific nature of the HPV11 E1–E2 protein–protein interaction that this class of inhibitors is antagonizing. Compound **23** also represents the first low nanomolar small molecule inhibitor of HPV11.

4. Conclusion

An extensive SAR study allowed us to improve the potency of our inhibitors by approximately 58-fold, as compared to the starting compound **6**. Moreover, compound **23** represents the first low nanomolar inhibitor of the HPV11 E1–E2 protein–protein interaction. In addition, using a combined NMR and computational chemistry approach, we were able to successfully determine the absolute stereochemistry of our active enantiomer and demonstrate that the activity resided in the 3*R*,4*S*,5*R* ('all-up') furan absolute configuration. This was later confirmed by X-ray co-crystallization studies.[11]

5. Experimental

5.1. General

All reactions were carried out under argon. Solvents and reagents were used as purchased. ^{1}H and ^{13}C NMR spectra were recorded at 400 and 100 MHz, respectively,

in DMSO-d_6 on a Bruker instrument and chemical shifts are referenced relative to internal DMSO set at 2.50 ppm (^{1}H) and 39.51 ppm (^{13}C). ES mass spectra were recorded on a Micromass Quattro II mass spectrometer. Column chromatography was performed either on silica gel (10–40 μm or 230–400 mesh ASTM, Merck) or preparative HPLC using a Partisil 10 ODS-3, C18 preparative column (50 cm × 22 mn). Analytical HPLC gradient chromatography was performed with acetonitrile and water containing 0.06% trifluoroacetic acid (TFA) using a Vydac C_{18} column (10 μm, 4.6 × 250 mm). Preparative chiral HPLC gradient chromatography was performed with acetonitrile and water containing 0.06% trifluoroacetic acid (TFA) using a Chiralcel OD column (10 μm, 20 × 250 mm).

5.2. Preparation of intermediate G

A solution of **F** (9.5 g, 75.4 mmol), malonic acid (15.7 g, 151 mmol), and piperidine (1.3 mL) in pyridine (40 mL) was refluxed overnight. The resulting mixture was allowed to cool to room temperature whereupon water (200 mL) was added. The mixture was acidified by the addition of concentrated HCl and allowed to stir for 1 h. The mixture was filtered and the solid washed with water. Drying under vacuum gave **G** as a yellow powder (12.8 g, 100%).

5.3. Preparation of intermediate H

A mixture of **G** (7.5 g, 44.6 mmol) and $Pd(OH)_2$ (500 mg) in ethanol was stirred under an atmosphere of hydrogen for 18 h. Filtering through glass microfiber and removal of solvent gave **H** as a white solid (7.0 g, 93%). Removal of solvent under reduced pressure gave **H** as a brown solid (3.72 g, 62%).

5.4. Preparation of intermediate I

Solid **H** (1 g, 5.88 mmol) was added in small portions to warm (75 °C) polyphosphoric acid (8.5 g). Heating was continued at 75 °C for 1 h after the addition was complete. Cooling to room temperature was followed by dilution with water and extraction with CH_2Cl_2 (3×). The combined organics were dried over $MgSO_4$ and concentrated. Flash chromatography (50% EtOAc in hexanes) gave **I** as a white solid (0.31 g, 35%).

5.5. Preparation of intermediate J

A solution of **I** (1.06 g, 6.97 mmol), 3,4-dibromobenzaldehyde (1.84 g, 6.97 mmol), and *p*-toluenesulfonic acid (100 mg) in benzene (25 mL) was refluxed for 24 h with azeotropic removal of water. Upon cooling and addition of ether (25 mL), a solid precipitated which was filtered to give **J** as a tan solid (1.35 g, 49%).

5.6. Preparation of intermediate K

To a solution of CrO_3 (50 mg, 0.50 mmol) in CH_2Cl_2 (15 mL) was added *tert*-butylhydroperoxide (2.6 mL of a 70% solution in water). After stirring for 2 min, **J** (1.0 g, 2.51 mmol) was added. After stirring for 18 h at room temperature the solution was diluted with CH_2Cl_2 and water, and extracted three times with small portions of CH_2Cl_2. The combined organics were dried over $MgSO_4$ and concentrated in vacuo. Trituration of the resulting solid with ether provided the corresponding diketone (0.61 g, 60%). The material so obtained (0.45 g) was dissolved in EtOH (15 mL) to which were added 30% H_2O_2 (0.38 mL) and one drop of 1 N NaOH. After stirring for 3 h the solution was filtered to give **K** as a yellow solid (421 mg, 90%).

5.7. Compound characterization

5.7.1. Compound 2. ^{1}H NMR (400 MHz, DMSO-d_6) δ (ppm): 8.13–8.10 (m, 4H), 7.49 (d, J = 8.5 Hz, 2H), 7.43 (d, J = 8.5 Hz, 2H), 7.03 (d, J = 8.1 Hz, 1H), 6.67 (d, J = 1.9 Hz, 1H), 6.65 (dd, J = 8.1, 1.9 Hz, 1H), 6.09 (s, 2H), 6.08 (d, J = 8.0 Hz, 2H), 4.26 (dd, J = 7.9, 7.9 Hz, 1H), 4.16 (d, J = 8.0 Hz, 1H); ^{13}C NMR (DMSO-d_6) δ: 197.8, 194.6, 173.4, 172.6, 147.3, 140.7, 139.0, 137.7, 137.6, 135.3, 132.5, 128.1, 128.0, 125.2, 124.5, 123.8, 120.6, 108.2, 107.5, 101.8, 84.1, 83.0, 52.1, 51.2; MS (ES−) *m*/*z*: 500.0 $(M-H)^-$, 518.1 $(M+18-H)^-$, 474.1; IR (KBr) ν 1788, 1713 cm^{-1} Anal. Calcd for $C_{27}H_{16}ClNO_7$: C, 64.62; H, 3.21; N, 2.79. Found: C, 64.50; H, 3.20; N, 2.88.

5.7.2. Compound 3. ^{1}H NMR (400 MHz, DMSO-d_6) δ (ppm): 8.18–8.09 (m, 4H), 7.58 (d, J = 8.0 Hz, 2H), 7.55 (d, J = 8.0 Hz, 2H), 7.07 (d, J = 8.3 Hz, 1H), 6.80 (d, J = 1.9 Hz, 1H), 6.74 (dd, J = 8.3, 1.9 Hz, 1H), 6.12 (s, 2H), 5.73 (d, J = 7.2 Hz, 1H), 4.27 (d, J = 9.8 Hz, 1H), 3.96 (dd, J = 9.8, 7.2 Hz, 1H); ^{13}C NMR (DMSO-d_6) δ: 198.0, 194.2, 174.1, 173.1, 148.2, 141.3, 141.1, 137.3, 137.2, 137.0, 134.5, 129.0, 127.3, 124.7, 124.6, 124.3, 120.7, 108.5, 107.9, 101.9, 84.2, 83.0, 55.0, 51.1; MS (ES−) *m*/*z*: 500.0 $(M-H)^-$, 518.0 $(M+18-H)^-$, 474.1 $(M+18-44)^-$; IR (KBr) ν 1743, 1708, 1687 cm^{-1}; Anal. Calcd for $C_{27}H_{16}ClNO_7$: C, 64.62; H, 3.21; N, 2.79. Found: C, 64.46; H, 3.27; N, 2.82.

5.7.3. Compound 4. ^{1}H NMR (400 MHz, DMSO-d_6) δ (ppm): 9.91 (s, 1H), 8.04–7.96 (m, 4H), 7.38 (d, J = 8.5 Hz, 2H), 7.31 (d, J = 8.5 Hz, 2H), 7.09 (d, J = 1.6 Hz, 1H), 6.89 (dd, J = 8.4, 1.6 Hz, 1H), 6.83 (d, J = 8.4 Hz, 1H), 5.96 (s, 2H), 5.71 (d, J = 5.9 Hz, 1H), 4.15 (d, J = 8.7 Hz, 1H), 3.65 (dd, J = 8.7, 5.9 Hz, 1H); ^{13}C NMR (DMSO-d_6) δ: 202.0, 199.8, 169.1, 167.5, 146.8, 143.8, 142.7, 138.8, 137.2, 136.1, 135.8, 133.5, 131.8, 127.7, 123.4, 112.5, 107.8, 102.0, 100.8, 85.1, 83.0, 62.0, 56.7; MS (ES−) *m*/*z*: 518.1 $(M-H)^-$, (ES+) *m*/*z*: 520.0 $(M+H)^+$, 542.0 $(M+Na)^+$, 502.0 $(M-Na+2H)^+$; mp 204.2 °C; IR (KBr) ν 1744, 1707, 1660 cm^{-1}.

5.7.4. Compound 5. ^{1}H NMR (400 MHz, DMSO-d_6) δ (ppm): 10.15 (s, 1H), 7.98 (dd, J = 7.4, 7.4 Hz, 1H), 7.94 (d, J = 7.4 Hz, 1H), 7.87 (d, J = 7.4 Hz, 1H), 7.77 (dd, J = 7.4, 7.4 Hz, 1H), 7.58 (s, 1H), 7.49 (d, J = 8.4 Hz, 2H), 7.39 (d, J = 8.4 Hz, 2H), 6.76 (d, J = 8.43 Hz, 1H), 6.71 (d, J = 1.7 Hz, 1H), 6.51 (dd,

J = 8.3, 1.7 Hz, 1H), 6.02 (d, J = 5.4 Hz, 1H), (m, 1H), 5.96 (s, 2H), 4.32 (d, J = 8.8 Hz, 1H), 3.98 (dd, J = 8.8, 5.4 Hz, 1H); ^{13}C NMR (DMSO-d_6) δ: 200.0, 171.4, 168.4, 148.2, 146.9, 144, 137.4, 134.4, 133.8, 132.6, 131.8, 131.1, 127.9, 124.8, 123.6, 113.6, 107.8, 105.6, 102.4, 101.1, 88.4, 88.0, 53.0, 52.7; MS (ES−) m/z: 517.9 $(M-H)^-$, 473.9 $(M-CO_2)^-$; mp 157.6 °C; IR (KBr) ν 3296–2900, 1746, 1710, 1655 cm^{-1}.

5.7.5. Compound 6. ^{1}H NMR (400 MHz, DMSO-d_6) δ (ppm): 10.02 (s, 1H), 8.07–7.96 (m, 4H), 7.59 (d, J = 1.6 Hz, 1H), 7.52 (d, J = 8.6 Hz, 1H), 7.35 (dd, J = 8.3, 1.6 Hz, 1H), 7.06 (d, J = 1.9 Hz, 1H), 6.83 (d, J = 8.3 Hz, 1H), 6.73 (dd, J = 8.6, 1.9 Hz, 1H), 5.96 (s, 2H), 5.70 (d, J = 5.7 Hz, 1H), 4.13 (d, J = 8.6 Hz, 1H), 3.66 (dd, J = 8.9, 6.0 Hz, 1H); ^{13}C NMR (DMSO-d_6) δ: 201.7, 199.5, 168.7, 167.3, 146.7, 143.7, 142.7, 138.8, 138.5, 137.0, 135.7, 133.3, 130.4, 139.8, 129.7, 127.8, 126.2, 123.4, 123.3, 112.6, 107.7, 102.0, 100.7, 84.3, 83.0, 61.9, 56.2; MS (ES−) m/z: 552.1 $(M-H)^-$; HRMS (FAB) Calcd for $C_{27}H_{17}Cl_2NO_8$ $(M+Na)^+$: 576.0228. Found: 576.0228.

5.7.6. Compound 7. ^{1}H NMR (400 MHz, DMSO-d_6) δ (ppm): 10.1 (s, 1H), 8.07–7.97 (m, 4H), 7.60 (d, J = 2.0 Hz, 1H), 7.50 (t, J = 8.2 Hz, 3H), 7.36 (dd, J = 8.5, 2.0 Hz, 1H), 7.27 (t, J = 7.9 Hz, 2H), 7.01 (t, J = 7.5 Hz, 1H), 5.72 (d, J = 6.0 Hz, 1H), 4.16 (d, J = 8.0 Hz, 1H), 3.71 (dd, J = 8.7, 5.0 Hz, 1H); MS (ES+) m/z: 509.9, 511.9; HRMS (FAB) Calcd for $C_{26}H_{17}Cl_2NO_6$ $(M+Na)^+$: 532.0330. Found: 532.0328.

5.7.7. Compound 8. ^{1}H NMR (400 MHz, DMSO-d_6) δ (ppm): 8.16–8.03 (m, 4H), 7.85 (s, 1H), 7.72 (d, J = 1.9 Hz, 1H), 7.68 (d, J = 8.3 Hz, 1H), 7.47 (dd, J = 8.3, 1.9 Hz, 1H), 5.73 (d, J = 6.3 Hz, 1H), 4.10 (d, J = 8.9 Hz, 1H), 3.53 (dd, J = 8.7, 6. Hz, 1H), 1.22 (s, 9H); MS (ES−) m/z: 488.1, 490.0, 491.1; HRMS (FAB) Calcd for $C_{24}H_{20}Cl_2NO_6$ $(M+Na)^+$: 512.0643. Found: 512.0645.

5.7.8. Compound 9. ^{1}H NMR (400 MHz, DMSO-d_6) δ (ppm): 9.02 (dd, J = 7.3, 4.4 Hz, 1H), 8.00 (s, 1H), 7.97 (d, J = 7.6 Hz, 1H), 7.95 (t, J = 7.6 Hz, 1H), 7.87 (d, J = 7.6 Hz, 1H), 7.78 (t, J = 7.6 Hz, 1H), 7.66 (s, 1H), 7.60 (d, J = 8.5 Hz, 1H), 7.40 (d, J = 8.5 Hz, 1H), 7.22–7.15 (m, 3H), 6.67 (d, J = 7.7 Hz, 2H), 5.95 (d, J = 5.7 Hz, 1H), 4.28 (d, J = 8.6 Hz, 1H), 4.22 (dd, J = 15.1, 7.3 Hz, 1H), 3.94 (dd, J = 8.6, 5.7 Hz, 1H), 3.88 (dd, J = 15.1, 4.4 Hz, 1H); MS (ES+) m/z: 524.0, 526.0; HRMS (FAB) Calcd for $C_{27}H_{19}Cl_2NO_6$ $(M+H)^+$: 524.0667. Found: 524.0667.

5.7.9. Compound 10. ^{1}H NMR (400 MHz, DMSO-d_6) δ (ppm): 9.56 (s, 1H), 9.50 (s, 1H), 8.18 (d, J = 8.3 Hz, 1H), 8.09–8.00 (m, 4H),7.70 (s, 1H), 7.65 (d, J = 8.3 Hz, 1H), 7.47 (d, J = 8.3 Hz, 1H), 7.15 (t, J = 7.6 Hz, 1H), 6.95 (t, J = 7.6 Hz, 1H), 6.70 (d, J = 7.6 Hz, 1H), 5.78 (d, J = 6.0 Hz, 1H), 4.23 (d, J = 8.9 Hz, 1H), 3.73 (dd, J = 8.9, 6.0 Hz, 1H), 2.09 (s, 3H); MS (ES−) m/z: 565.0, 567.0; HRMS (FAB) Calcd for $C_{28}H_{20}Cl_2N_2O_7$ $(M+Na)^+$: 589.0545. Found: 589.0545.

5.7.10. Compound 11. ^{1}H NMR (400 MHz, DMSO-d_6) δ (ppm): 10.18 (s, 1H), 9.80 (s, 1H) 8.06–7.96 (m, 4H), 7.64 (s, 1H), 7.59 (d, J = 1.6 Hz, 1H), 7.48 (d, J = 8.3 Hz, 2H), 7.35 (dd, J = 8.3, 1.6 Hz, 1H), 7.17–7.11 (m, 2H), 5.69 (d, J = 5.7 Hz, 1H), 4.14 (d, J = 8.6 Hz, 1H), 3.72 (dd, J = 8.6, 5.7 Hz, 1H), 2.01 (s, 3H); MS (ES−) m/z: 565.1, 567.1; HRMS (FAB) Calcd for $C_{28}H_{20}Cl_2N_2O_7$ $(M+Na)^+$: 589.0545. Found: 589.0545. IR (KBr) ν 3567, 3267, 3189, 3071, 1742, 1707, 1666, 1592, 1551, 1483, 1393 cm^{-1}.

5.7.11. Compound 12. ^{1}H NMR (400 MHz, DMSO-d_6) δ (ppm): 10.12 (s, 1H), 9.85 (s, 1H) 8.04–8.00 (m, 4H), 7.60 (s, 1H), 7.51–7.44 (m, 3H), 7.36–7.35 (m, 2H), 5.70 (br d, 1H), 4.16 (d, J = 8.6 Hz, 1H), 3.68 (m, 1H), 2.00 (s, 3H); MS (ES+) m/z: 567.0, 569.1; HRMS (FAB) Calcd for $C_{28}H_{20}Cl_2N_2O_7$ $(M+Na)^+$: 589.0545. Found: 589.0545.

5.7.12. Compound 13. ^{1}H NMR (400 MHz, DMSO-d_6) δ (ppm): 10.53 (s, 1H), 8.10–7.97 (m, 4H), 7.89 (d, J = 8.6 Hz, 2H), 7.63 (d, J = 8.9 Hz, 2H), 7.58–7.57 (m, 1H), 7.48 (d, J = 8.3 Hz, 1H), 7.35–7.33 (m, 1H), 5.72 (d, J = 5.7 Hz, 1H), 4.17 (d, J = 8.6 Hz, 1H), 3.80 (dd, J = 8.6, 5.7 Hz, 1H), 2.45 (s, 3H); MS (ES+) m/z: 552.1, 554.1; HRMS (FAB) Calcd for $C_{28}H_{19}Cl_2NO_7$ $(M+Na)^+$: 574.0436. Found: 574.0436. IR (KBr) ν 2900, 1710, 1591 cm^{-1}.

5.7.13. Compound 14. ^{1}H NMR (400 MHz, DMSO-d_6) δ (ppm): 10.34 (s, 1H), 9.51 (s, 1H), 8.11–7.96 (m, 6H), 7.66 (d, J = 8.4 Hz, 2H), 7.61 (d, J = 1.8 Hz, 2H), 7.50 (d, J = 8.4 Hz, 1H), 7.37 (dd, J = 8.4, 1.8 Hz, 1H), 5.74 (d, J = 5.7 Hz, 1H), 4.19 (d, J = 8.6 Hz, 1H), 3.76 (dd, J = 8.6, 5.7 Hz, 1H); MS (ES−) m/z: 592.0, 594.0; HRMS (FAB) Calcd for $C_{28}H_{17}Cl_2N_3O_6S$ $(M+Na)^+$: 616.0112. Found: 616.0112.

5.7.14. Compound 15. ^{1}H NMR (400 MHz, DMSO-d_6) δ (ppm): 9.90 (s, 1H), 8.05–7.95 (m, 4H), 7.60 (d, J = 1.9 Hz, 1H), 7.50 (d, J = 8.3 Hz, 1H) 7.40–7.30 (m, 1H), 7.30 (d, J = 9 Hz, 2H), 6.85 (d, J = 9 Hz, 2H), 5.70 (d, J = 5.7 Hz, 1H), 4.13 (d, J = 8.6 Hz, 1H), 3.74–3.67 (m, 4H), 3.62–3.60 (m, 1H), 3.04–3.02 (m, 4H); MS (ES−) m/z: 593.0, 595.0; HRMS (FAB) Calcd for $C_{30}H_{24}Cl_2N_2O_7$ $(M+Na)^+$: 617.0858. Found: 617.0858.

5.7.15. Compound 16. ^{1}H NMR (400 MHz, DMSO-d_6) δ (ppm): 8.98 (d, J = 8.1 Hz, 1H), 7.97 (s, 1H), 7.99–7.90 (m, 2H), 7.85 (d, J = 7.1 Hz, 1H), 7.76 (t, J = 7.1 Hz, 1H) 7.57 (d, J = 1.6 Hz, 1H), 7.47 (d, J = 8.3 Hz, 1H), 7.32 (dd, J = 8.3, 1.6 Hz, 1H), 7.20–7.19 (m, 3H), 6.64 (d, J = 7.1 Hz, 2H), 5.91 (d, J = 5.3 Hz, 1H), 4.69 (m, 1H), 4.26 (d, J = 8.9 Hz, 1H), 3.92 (dd, J = 8.9, 5.3 Hz, 1H), 1.23 (d, J = 7.0 Hz, 3H); MS (ES−) m/z: 536.1, 538.1; HRMS (FAB) Calcd for $C_{28}H_{21}Cl_2NO_6$ $(M+H)^+$: 538.0824. Found: 538.0826.

5.7.16. Compound 17. ^{1}H NMR (400 MHz, DMSO-d_6) δ (ppm): 8.85 (d, J = 8.1 Hz, 1H), 7.96 (t, J = 7.3 Hz, 1H), 7.92 (s, 1H), 7.90 (d, J = 7.3 Hz, 1H), 7.85 (d,

$J = 7.6$ Hz, 1H), 7.76 (t, $J = 7.6$ Hz, 1H) 7.70 (d, $J = 8.7$ Hz, 1H), 7.68 (s, 1H), 7.44 (d, $J = 8.6$ Hz, 1H), 7.29 (t, $J = 7.2$ Hz, 2H), 7.23 (d, $J = 7.2$ Hz, 1H), 7.17 (d, $J = 7.2$ Hz, 2H), 5.98 (d, $J = 5.1$ Hz, 1H), 4.60 (m, 1H), 4.23 (d, $J = 8.7$ Hz, 1H), 3.95 (dd, $J = 8.7$, 5.2 Hz, 1H), 0.74 (d, $J = 7.0$ Hz, 3H); MS (ES+) *m/z*: 538.1, 540.1; HRMS (FAB) Calcd for $C_{28}H_{21}Cl_2NO_6$ $(M+H)^+$: 538.0824. Found: 538.0826.

5.7.17. Compound 18. ^{1}H NMR (400 MHz, DMSO-d_6) δ (ppm): 10.4 (s, 1H), 9.51 (s, 1H), 8.05 (d, $J = 8.3$ Hz, 1H), 8.00–7.60 (m, 6H), 7.53 (d, $J = 8.4$ Hz, 1H), 7.37 (d, $J = 8.4$ Hz, 1H), 5.74 (br s, 1H), 4.17 (br d, $J = 8.3$ Hz, 1H), 3.76 (br s, 1H), 2.61 (s, 3H); MS (ES−) *m/z*: 606.1, 608.0, 609.0; HRMS (FAB) Calcd for $C_{29}H_{19}Cl_2N_3O_6S$ $(M+Na)^+$: 630.0269. Found: 630.0269.

5.7.18. Compound 19. ^{1}H NMR (400 MHz, DMSO-d_6) δ (ppm): 10.12 (s, 1H), 8.12–7.69 (m, 6H), 7.4 (d, $J = 7.3$ Hz, 1H), 7.00 (d, $J = 8.5$ Hz, 2H), 6.82 (d, $J = 8.5$ Hz, 2H), 5.99 (br s, 1H), 4.30 (br d, $J = 9.0$ Hz, 1H), 4.00 (br s, 1H), 3.70 (m, 4H), 3.02–3.01 (m, 4H); MS (ES+) *m/z*: 582.8, 584.8, 586.8; HRMS (FAB) Calcd for $C_{30}H_{24}Br_2N_2O_7$ $(M+Na)^+$: 704.9847. Found: 704.9847.

5.7.19. Compound 20. ^{1}H NMR (400 MHz, DMSO-d_6) δ (ppm): 10.12 (s, 1H), 8.12–7.69 (m, 6H), 7.4 (d, $J = 7.3$ Hz, 1H), 7.00 (d, $J = 8.5$ Hz, 2H), 6.81 (d, $J = 8.5$ Hz, 2H), 6.0 (d, $J = 5.4$ Hz, 1H), 4.30 (d, $J = 8.6$ Hz, 1H), 4.00 (dd, $J = 8.6$, 5.4 Hz, 1H), 3.70 (m, 4H), 3.01 (m, 4H); MS (ES−) *m/z*: 681.0, 683.0, 685.0; HRMS (FAB) Calcd for $C_{30}H_{24}Br_2N_2O_7$ $(M+Na)^+$: 704.9847. Found: 704.9847.

5.7.20. Compound 21. ^{1}H NMR (400 MHz, DMSO-d_6) δ (ppm): 10.12 (br s, 1H), 8.14–7.65 (m, 6H), 7.4 (d, $J = 7.3$ Hz, 1H), 7.00 (d, $J = 8.9$ Hz, 2H), 6.81 (d, $J = 8.9$ Hz, 2H), 6.0 (d, $J = 5.4$ Hz, 1H), 4.30 (br d, $J = 9.0$ Hz, 1H), 4.00 (br s, 1H), 3.70 (m, 4H), 3.01 (m, 4H); MS (ES−) *m/z*: 681.0, 683.0, 684.0; HRMS (FAB) Calcd for $C_{30}H_{24}Br_2N_2O_7$ $(M+Na)^+$: 704.9847. Found: 704.9847.

5.7.21. Compound 22. ^{1}H NMR (400 MHz, DMSO-d_6) δ (ppm): 9.25 (s, 1H), 7.72 (d, $J = 2.0$ Hz, 1H), 7.58 (d, $J = 8.3$ Hz, 1H), 7.34 (s, 1H), 7.27 (dd, $J = 2.0$, 8.3. Hz, 1H), 7.04 (d, $J = 9.2$ Hz, 2H), 6.76 (d, $J = 9.2$ Hz, 2H), 5.63 (d, $J = 6.1$ Hz, 1H), 4.35 (d, $J = 8.6$, 1H), 3.81 (dd, $J = 6.1$, 8.6 Hz, 1H), 3.66 (br s, 4H), 2.96 (br s, 4H), 2.66 (s, 3H); MS (ES−) *m/z*: 700.9, 702.9, 704.8.

5.7.22. Compound 23. ^{1}H NMR (400 MHz, DMSO-d_6) δ (ppm): 10.1 (s, 1H), 7.85 (s, 1H), 7.65 (d, $J = 8.2$ Hz, 1H), 7.40 (d, $J = 8.2$. Hz, 1H), 7.35 (s, 1H), 6.95 (d, $J = 9.0$ Hz, 2H), 6.85 (d, $J = 9.0$ Hz, 2H), 5.95 (d, $J = 6.0$ Hz, 1H), 4.31 (d, $J = 8.5$ Hz, 1H), 4.04 (dd, $J = 6.0$, 8.5 Hz, 1H), 3.87 (br s, 4H), 3.05 (br s, 4H), 2.70 (s, 3H); MS (ES−) *m/z*: 700.9, 702.9, 704.8; HRMS (FAB) Calcd for $C_{29}H_{23}Br_2N_2O_7S$ $(M-H)^-$: 700.9592. Found: 700.9598.

5.8. NMR methods

1D NOE and 2D COSY, ROESY, HMQC, and HMBC experiments were recorded at 300 K on a Bruker DRX400 spectrometer equipped with a gradient triple resonance probe using the standard pulse sequences provided by the manufacturer. The ROESY experiments for compounds **16** and **17** were recorded with a 300 ms spin-lock period. The 2D data sets were typically acquired with 2048 points in t_2, 256 points in t_1, and 128 scans. The data were processed and analyzed using XWinNMR software (Bruker Canada, Milton, Ontario).

5.9. Computational chemistry methods

The two hydroxylactone derivatives **16** and **17** were studied by molecular mechanics in order to determine their conformational preferences *in-silico*. A systematic conformational search around key single bonds (a–e, shown below) was performed for each compound using the MMFF94 forcefield within the MOE software package (Chemical Computing Group Inc., Montreal, Canada). The calculations were performed in vacuo using a distance dependent dielectric constant and without non-bonded cutoffs. The different angles (**a**–**e**) were rotated systematically while the remaining parameters were allowed to relax. Specifically, angle **a** was varied by 120°, angle **b** by 60°, angle **c** by 15°, angle **d** by 15°, and angle **e** by 120° to generate ultimately 5393 points. Symmetry was exploited when possible. Each point was then gradient minimized and redundant structures were eliminated (RMSD < 1 Å), leading to the identification of a series of distinct low energy conformations. The five lowest energy conformations found for each diastereoisomer were selected (supplementary materials). In addition, the distances between the center of the 3,4-dichlorophenyl ring and both the centers of the benzyl ring and of the methyl moiety were measured for these five lowest energy conformations and tabulated.

5.10. In vitro assay

The activity of all the inhibitors was determined using a E1–E2-ori-complex formation assay as previously described.[8] Each reported IC_{50} value represents the mean of at least three determinations. In addition, all inhibitors were tested and found inactive (data not shown) in a mechanistically related scintillation proximity assay (SPA) that measures binding of SV40 large T antigen to its cognate origin, demonstrating that they do not interfere with the scintillation proximity detection procedure or bind promiscuously to DNA or protein.[8]

Acknowledgments

The authors thank Norman Aubry, Colette Boucher, Michael Little, and Serge Valois for excellent analytical support. We also acknowledge Dr. Yong Wang and René Coulombe for the crystallographic work, Louise Thauvette for protein production and purification, and

Ewald Welchner for IC_{50} determination. Finally we extend our gratitude to Drs. Paul Anderson, Jacques Archambault, Michael Bös, and Michael Cordingley for encouragement and support.

Supplementary data

Supplementary data associated with this article can be found, in the online version, at doi:10.1016/j.bmc.2007.01.036.

References and notes

1. Shah, K. V.; Howley, P. M. In *Fields Virology*, 3rd ed.; Lippincott-Raven Publishers: Philadadelphia, 1996; pp 2077–2109.
2. Hanna, E.; Bachmann, G. *Expert Opin. Biol. Ther.* **2006**, *6*, 1223–1227.
3. Beutner, K. R.; Ferenczy, A. *Am. J. Med.* **1997**, *102*, 28–37.
4. Beutner, K. R.; Tyring, S. K.; Trofatter, K. F., Jr.; Douglas, J. M., Jr.; Spruance, S.; Owens, M. L.; Fox, T. L.; Hougham, A. J.; Schmitt, K. A. *Antimicrob. Agents Chemother.* **1998**, *42*, 789–794.
5. Howley, P. M. In *Fields Virology*, 3rd ed.; Lippincott-Raven Publishers: Philadadelphia, 1996; pp 2045–2076.
6. Abbate, E. A.; Berger, J. M.; Botchan, M. R. *Gene and Development* **2004**, *18*, 1981–1996.
7. Yoakim, C.; Ogilvie, W. W.; Goudreau, N.; Naud, J.; Haché, B.; O'Meara, J. A.; Cordingley, M. G.; Archambault, J.; White, P. W. *Bioorg. Med. Chem. Lett.* **2003**, *13*, 2539–2541.
8. White, P. W.; Titolo, S.; Brault, K.; Thauvette, L.; Pelletier, A.; Welchner, E.; Bourgon, L.; Doyon, L.; Ogilvie, W. W.; Yoakim, C.; Cordingley, M. G.; Archambault, J. *J. Biol. Chem.* **2003**, *278*, 26765–26772.
9. White, P. W.; Pelletier, A.; Brault, K.; Titolo, S.; Welchner, E.; Thauvette, L.; Fazekas, M.; Cordingley, M. G.; Archambault, J. *J. Biol. Chem.* **2001**, *25*, 22426–22438.
10. Yoakim, C.; Goudreau, N.; McGibbon, G. A.; O'Meara, J. A.; White, P. W.; Ogilvie, W. W. *Helvetica Chim. Acta* **2003**, *86*, 3427–3444.
11. Wang, Y.; Coulombe, R.; Cameron, D. R.; Thauvette, L.; Massariol, M.-J.; Amon, L. M.; Fink, D.; Titolo, S.; Welchner, E.; Yoakim, C.; Archambault, J.; White, P. W. *J. Biol. Chem.* **2004**, *8*, 6976–6985.